CORRESPONDING AUTHOR INFO

Name: Iker Aranjuelo

Instituto de Agrobiotecnología, Universidad Pública de Navarra-CSIC-Gobierno de Navarra, Campus de Arrosadia, E-31192-Mutilva Baja, Spain.

Fax: +0034 948 232191

E-mail address: iker.aranjuelo@gmail.com

Does ear C sink strength contribute to overcoming photosynthetic acclimation of wheat plants exposed to elevated CO_2?

Iker Aranjuelo[1,2*], Llorenç Cabrera-Bosquet[2], Rosa Morcuende[4], Jean Christophe Avice[3], Salvador Nogués[2], José Luis Araus[2], Rafael Martínez-Carrasco[4], Pilar Pérez[4]

[1] Instituto de Agrobiotecnología, Universidad Pública de Navarra-CSIC-Gobierno de Navarra, Campus de Arrosadia, E-31192-Mutilva Baja, Spain.

[2] Unitat de Fisologia Vegetal, Facultat de Biologia, Universitat de Barcelona, Diagonal 645, 08028, Barcelona, Spain.

[3] INRA, UMR INRA/UCBN 950 Ecophysiologie Végétale, Agronomie et Nutritions NCS, IFR 146 ICORE, Institut de Biologie Fondamentale et Appliquée, Université de Caen Basse-Normandie, F–14032 Caen, France.

[4] Institute of Natural Resources and Agrobiology of Salamanca, CSIC, Apartado 257, E-37071 Salamanca, Spain.

Running title: Ear C sink strength under elevated CO_2

Date of submission: 26th-Novemeber 2010

Number of tables: 3

Number of figures: 6

Corresponding author:

Name: Iker Aranjuelo

Present address: Instituto de Agrobiotecnología, Universidad Pública de Navarra-CSIC-Gobierno de Navarra, Campus de Arrosadia, E-31192-Mutilva Baja, Spain.

Phone: +0034 948 168000

Fax: +0034 948 232191

E-mail address: iker.aranjuelo@gmail.com

Abstract

Wheat plants (*Triticum durum* Desf., cv. Regallo) were grown in the field to study the effects of contrasting [CO_2] conditions (700 *versus* 370 μmol mol^{-1}) on growth, photosynthetic performance and C management during the post-anthesis period. The ambient $^{13}C/^{12}C$ isotopic composition ($\delta^{13}C$) of air CO_2 was changed from -10.2 ‰ in ambient [CO_2] to -23.6 ‰ under elevated [CO_2] between the 7^{th} and the 14^{th} day after anthesis in order to study C assimilation and partitioning between leaves and ears. Elevated [CO_2] had no significant effect on biomass production and grain filling, and caused an accumulation of C compounds in leaves. This was accompanied by an up-regulation of phosphoglycerate mutase and ATP synthase protein content, together with a down-regulation of adenosine diphosphate glucose pyrophosphatase protein. Growth in elevated [CO_2] negatively affected Rubisco and Rubisco activase protein content and induced photosynthetic down-regulation. CO_2 enrichment caused a specific decrease in Rubisco content, together with decreases in the amino acid and total N content of leaves. The C labelling revealed that in flag leaves, part of the C fixed during grain filling was stored as starch and structural C compounds whereas the rest of the labelled C (mainly in the form of soluble sugars) was completely respired 48 h after the end of labelling. Although $\delta^{13}C$ of ear total organic matter (TOM) and respired CO_2 did not detect labelled C, soluble sugar $\delta^{13}C$ revealed that a small amount of labelled C reached the ear. The $^{12}CO_2$ labelling suggests that during the beginning of post-anthesis, the ear did not contribute to overcome flag leaf carbohydrate accumulation with a consequent effect on protein expression and photosynthetic acclimation.

Keywords: C management, elevated CO_2, photosynthetic acclimation, proteomic characterisation, Rubisco, stable isotopes.

Abbreviations: **A_{370}**, photosynthesis determined at 370 μmol mol^{-1} CO_2; **A_{700}**, photosynthesis determined at 700 μmol mol^{-1} CO_2; **ADPG**, ADPglucose; **AGPPase**, adenosine diphosphate glucose pyrophosphatase; **CA**, Carbonic anhydrase; **Ci_{370}**, intercellular [CO_2] determined at 370 μmol mol^{-1} CO_2; **Ci_{700}**, intercellular [CO_2] determined at 700 μmol mol^{-1} CO_2; **DM**, dry matter; **gs_{370}**, stomatal conductance determined at 370 μmol mol^{-1} CO_2; **gs_{700}**, stomatal conductance determined at 700 μmol mol^{-1} CO_2; **IRGA**, infrared gas analyser; **k_{cat}**, overall enzyme catalytic rate; **PAR,** Photosynthetically active radiation; **PDB,** Pee Dee Belemnite; **PGAM**, Phosphoglycerate mutase; **PPFD**, photosynthetic photon flux density; **RuBP**, Ribulose bis-phospahte; **R,** dark respiration; **T_0**, immediately after the end of labelling; **T_1**, 24 h after the end of labelling; **T_2**, 48 h after the end of labelling; **TOM**, total organic matter; **TSP**, total soluble proteins; **TSS**, total soluble sugar; **$\delta^{13}C$**, ^{13}C isotopic composition; $\delta^{13}C_a$, air ^{13}C isotopic composition; $\delta^{13}C_p$, plant ^{13}C isotopic composition; **Δ,** C isotope discrimination; **2-PGA**, 2-phosphoglycerate; **3-PGA**, 3-phosphoglycerate.

Introduction

The global atmospheric concentration of carbon dioxide ($[CO_2]$) has increased from about 280 μmol mol^{-1} during the pre-industrial period to 388.5 μmol mol^{-1} in 2010 (Dr. Pieter Tans, NOAA/ESRL, www.esrl.noaa.gov/gmd/ccgg/ trends/) and is expected to reach 700 μmol mol^{-1} by the end of this century (Prentice *et al.*, 2001). The primary effects of increased $[CO_2]$ on plants include (i) increased plant biomass and (ii) leaf net photosynthetic rates, and (iii) decreased stomatal conductance (Long *et al.*, 2004; Nowak *et al.*, 2004; Ainsworth and Long 2005). The biochemical basis for the leaf CO_2 assimilation response to increased atmospheric $[CO_2]$ is well established (Farquhar *et al.*, 1980). At concentrations below 600 μmol mol^{-1} CO_2, leaf CO_2 assimilation increases because Rubisco carboxylation is enhanced by increased substrate availability and the suppression of competitive Rubisco oxygenation (Ellsworth *et al.*, 2004). Although the initial stimulation of net photosynthesis associated with elevated $[CO_2]$ is sometimes retained (Davey *et al.*, 2006), some species fail to sustain the initial, maximal stimulation (Aranjuelo *et al.*, 2005a; Martínez-Carrasco *et al.*, 2005; Pérez *et al.*, 2007; Alonso *et al.*, 2009; Gutiérrez *et al.*, 2009), a phenomenon called photosynthetic acclimation or down-regulation.

Stomatal limitations reduce photosynthesis due to depletion of intercellular $[CO_2]$ (C_i) as a result of stomatal closure (Naumburg *et al.*, 2004), i.e. a reduced supply of CO_2 to the photosynthetic apparatus within leaves. Non-stomatal limitations reduce photosynthesis due to reduced photosynthetic electron transport (Aranjuelo *et al.*, 2008) or decreased Rubisco carboxylation of RuBP (Stitt and Krapp, 1999; Long *et al.*, 2004; Aranjuelo *et al.*, 2005a).

Decreased Rubisco carboxylation occurs through two basic mechanisms: one that involves C source/sink relationships and a second that involves N allocation. Enhanced leaf C content caused by greater photosynthetic rates in plants exposed to elevated [CO_2] induces repression of the expression of genes coding for photosynthetic proteins, leading to a down-regulation of photosynthetic capacity (Moore *et al*., 1999; Jifon and Wolfe, 2002). The increased leaf C concentration can occur at the leaf level, or it may involve whole plant source/sink relationships. From this point of view, the reduction in leaf photosynthetic rates would be caused by a plant's ability to develop new sinks or to expand the storage capacity or growth rate of existing sinks (Lewis *et al*., 2002; Aranjuelo *et al*., 2009a). In this sense, when plants exposed to elevated [CO_2] have limitations on increasing C sink strength, plants decrease their photosynthetic activity to balance C source activity and sink capacity (Thomas and Strain, 1991). The second basic mechanism leading to down-regulation is reduced Rubisco content caused by non-selective decreases in leaf N content (Ellsworth *et al*., 2004; Aranjuelo *et al*., 2005a) or by reallocation of N within the plant (Nakano *et al*., 1997). In both cases, reduced leaf N decreases Rubisco content.

Leaf carbohydrate accumulation is determined by the C source (photosynthesis) and sink balance (i.e. growth, respiration and partitioning to other organs) (Aranjuelo *et al*., 2009a). Despite the relevance of C loss through respiration, little attention has been given to this topic in cereals (Araus *et al*., 1993; Bort *et al*., 1996). Previous studies conducted in wheat and other cereals by Araus *et al.* (1993) revealed that dark respiration *(R)* in ears during grain filling ranges from 44-63 % of the gross photosynthesis (net CO_2 assimilation plus dark respiration), 12-20 days after ear emergence. Furthermore, as observed in recent studies (Aranjuelo *et al*., 2009a), the "ability" to respire recently assimilated C may

contribute towards preventing carbohydrate build-up and consequently to the avoidance of photosynthetic acclimation. In cereals like wheat, the ear comprises a very important C sink, especially during grain filling (Schnyder, 1993). In wheat, grain filling is sustained by photoassimilates (i) from the flag leaf (Evans *et al*. 1975), (ii) from C fixed by the ear itself (Tambussi *et al*. 2007) and (iii) from C remobilised from the stem internodes that was assimilated before anthesis (Gebbing and Schnyder 1999).

As revealed by previous studies conducted with plants exposed to elevated [CO_2] conditions (Körner *et al.*, 2005; von Felten *et al.*, 2007; Aranjuelo *et al.*, 2008; 2009a), stable C isotope tracers are a key tool to study C management and its implications in photosynthetic performance. One of the difficulties of analysing the processes involved in C metabolism (photosynthesis, respiration, allocation and partitioning) is measuring the different processes simultaneously in the same experiment (Amthor, 2001). The lack of studies analysing the loss of photoassimilates by respiration during grain filling, underscores the importance of examining this further. Labelling with $^{13}C/^{12}C$ enables the characterisation of assimilated C and its further partitioning into different organs (Nogués *et al.*, 2004; Aranjuelo *et al.*, 2009ab). C allocation and partitioning can be studied further by analysing the isotopic composition of soluble sugars (especially sucrose, glucose, etc.) (Körner *et al.*, 2005; Kodama *et al.*, 2010).

The aim of this paper was to determine the role of ears as major C sinks during grain filling and its effect on the leaf C content, photosynthetic acclimation and plant growth of wheat plants exposed to elevated [CO_2] under near field conditions. The significance for grain filling of C management (photosynthesis, respiration, allocation and partitioning) in

wheat under elevated [CO_2] was assessed through $^{12}CO_2$ labelling carried out in greenhouses located in the field. $^{12}CO_2$ labelling was conducted at the plant level to gain a better understanding of C management in the whole plant. Furthermore, a biochemical and proteomic characterisation was conducted to extend our knowledge of the effects of elevated [CO_2] on the expression profile of proteins other than the most extensively characterised Rubisco.

Materials and Methods

Experimental design

The experiment was conducted at Muñovela, the experimental farm of the Institute of Natural Resources and Agrobiology of Salamanca, CSIC (Salamanca, Spain). Durum wheat (*Triticum durum* Desf. cv. Regallo) was sown at a rate of 200 kg ha^{-1} and 0.13 row spacing on 29 October 2007. Before sowing, 60 kg ha^{-1} each of P and K (as P_2O_5 and K_2O, respectively) were added. An application of nitrogen fertiliser [$Ca(NO_3)_2$] as an aqueous solution was made by hand at 140 kg ha^{-1}, on 15 February 2008. The crop was watered weekly with a drip irrigation system, providing the amount of water required to equal potential evapotranspiration. After seedling emergence, six greenhouses (Aranjuelo *et al.*, 2005b; Pérez *et al.*, 2005; Gutiérrez *et al.*, 2009), based on those described by Rawson *et al.* (1995), were erected over the crop. The greenhouses were 9 m long, 2.2 m wide and 1.7 m high at the ridge. For the roof, UV-stable polyethylene sheet was used. This material has good transmission of photosynthetically active and UV radiation, adequately mimicking outdoor conditions. Photosynthetically active radiation (PAR) at mid-morning was 1020 ±

187 μmol m^{-2} s^{-1} outdoors, whereas inside the greenhouses the PAR was 825 ± 113 μmol m^{-2} s^{-1}. Three greenhouses were kept at ambient [CO_2] (370 μmol mol^{-1}), while in the other three atmospheric [CO_2] was increased to 700 μmol mol^{-1} (elevated [CO_2]) by injecting pure CO_2 at the two inlet fans during the light hours. CO_2 was not elevated during the night because little or no effect on dark respiration has been reported (Davey *et al.*, 2004). The atmospheric CO_2 concentration inside the greenhouses was continuously monitored at the plant level and regulated by PID controllers (Aranjuelo *et al.*, 2005a). Temperature and humidity were measured with sensors (HMD50; Vaisala, Helsinki, Finland) attached to a computer through analogue-digital convertors (Microlink 751, Biodata Ltd, Manchester, UK). Supplementary Figure S1 shows the temperature and relative humidity inside the greenhouses during the experiment.

To analyse C allocation and partitioning in the plants, during the first week after anthesis and coinciding with the period of largest photoassimilate contribution to grain filling (Schnyder *et al.*, 2003), C labelling was conducted over one week via modification of the isotopic composition of the air ^{13}C ($\delta^{13}C$). During the C labelling period, the plants exposed to elevated [CO_2] conditions were grown in an environment where the $\delta^{13}C$ of the greenhouses was deliberately modified (-23.6 ± 0.4‰) to distinguish it from the $\delta^{13}C$ of elevated [CO_2] (-20.1 ± 0.4‰) during the previous period. Air $\delta^{13}C$ in the ambient [CO_2] was -10.2 ± 0.4‰. The CO_2 was provided by Air Liquide (Valladolid, Spain). See below for details on air $\delta^{13}C$ collection and measurements. All the determinations, with the exception of C labelling derived parameters, were conducted on the last day of the

experiment, 14 days after anthesis. Isotopic characterisation data was performed at the end of 7 days labelling (T_0; two weeks after anthesis), and 24 h (T_1) and 48 h (T_2) later.

Gas exchange and plant growth

Gas exchange of leaves was recorded in the central segment of flag leaves between 3 and 8 h after the start of the photoperiod. Measurements were carried out with an air flow rate of 300 mL min^{-1}, 1500 µmol m^{-2} s^{-1} irradiance, and a 1.6 ± 0.23 kPa vapour pressure deficit, using a 1.7 cm^2-window leaf chamber connected to a portable infrared gas analyser (CIRAS-2, PP Systems, Hitchin, Herts, UK) with differential operation in an open system. Temperature was kept at 25 ºC with the Peltier system of the analyser. Photosynthesis was recorded at 370 and 700 µmol mol^{-1} CO_2.

To determine dry matter accumulation, the number of shoots in 0.5 m of two adjacent rows was counted, five consecutive shoots were harvested from each of the rows and the dry weight of leaves, stems and ears was recorded after drying in an oven at 60 ºC for 48 h. This allowed the results to be expressed on a ground area basis.

Rubisco protein, amino acids and Rubisco activity

At mid-morning samples consisting of four leaves were harvested and rapidly plunged in situ into liquid nitrogen and then stored at -80 ºC until analysed. The fresh weight, leaf area and chlorophyll content of subsamples of frozen leaves were determined as described (Pérez *et al.*, 2005).This allowed the results to be expressed on a leaf area basis.

Total amino acids were determined spectrophotometrically by the ninhydrin method according to Hare (1977) as described by Morcuende *et al.* (2004). The soluble proteins were extracted by grinding frozen leaf subsamples to a fine powder in 50 mM Tricine buffer (pH 8.0), 2 mM EDTA, 10 mM NaCl, 5 mM $MgCl_2$, 75 mM sucrose, 5 mM ε-aminocaproic acid, 2 mM benzamidine, 8 mM β-mercaptoethanol and 2 mM PMSF for 5 min on ice. This was followed by centrifugation at 12,500 g for 30 min at 4 °C. Protein concentrations were measured in the decanted supernatant (Bradford, 1976), and five volumes of cold acetone were added to an aliquot containing 200 mg of protein, which was left overnight in the freezer. The samples were then centrifuged at 12,000 *g* for 15 min at 4 ºC. The acetone was allowed to evaporate off. The precipitates were dissolved in 65 mM Tris-HCl (pH 6.8), 3 M sucrose, 0.6 M β-mercaptoethanol, 5% sodium dodecylsulphate (SDS, w:v) and 0.01% bromophenol blue at 96 ºC for 7 min. The samples were then cooled to room temperature and aliquots of the SDS-dissociated extracts, containing 15 µg of protein, were loaded onto a 12.5% SDS-polyacrylamide gel (Mini-Protean 3 Cell, Bio Rad). This protein amount was within the range of linear response of optical density to the concentration of a BSA standard (66 kDa), according to previous calibration measurements. The solubilised proteins were separated by SDS-polyacrylamide gel electrophoresis (PAGE; Laemmli, 1970) using a 0.75 mm thick gel (12.5% resolving, 4% stacking). Electrophoresis was carried out at room temperature at a constant 200 V. The gels were fixed in 500:150:75 (v:v:v) water-methanol-acetic acid mixture for 75 min, stained in EZ Blue Gel Staining (Sigma) solution for 2 h, and subsequently rinsed in water to remove excess stain. Finally, the gels were scanned with a high-resolution scanner (Scanjet G4050, Hewlett Packard, Spain) and the amount of Rubisco subunits was determined by

densitometry with image analysis software (Image Quant, Molecular Dynamics, GE Healthcare, Spain).

For Rubisco initial and total activity assays, a NADH-coupled spectrophotometric procedure was followed (Pérez *et al.*, 2005). To estimate the k_{cat}, total Rubisco activity was divided by the number of enzyme active sites, which was obtained by multiplying the number of moles of Rubisco by 8.

Soluble sugar and starch content analyses

For sugar extraction, plant samples were lyophilised and then ground to a fine powder (<10 μm). About 50 mg of the fine powder were suspended in 1 mL of distilled water in an Eppendorf tube (Eppendorf Scientific, Hamburg, Germany), mixed, and then centrifuged at 12,000 g for 5 min at 5 ºC. After centrifugation, the supernatant was used for sugar quantification, whereas the pellet was stored at -80 ºC for further starch analyses. The supernatant was heated during 3 min at 100 ºC and afterward the solution was put on ice for 3 min. The supernatant containing the total soluble sugar (TSS) fraction was centrifuged at 12,000 g for 5 min at 5 ºC (Nogués *et al.*, 2004). The supernatant was used for quantification of the individual sugars. Soluble sugar samples were purified using a solid phase extraction pre-column (Oasis MCX 3cc, Waters). Sugar content was analysed using a Waters 600 high performance liquid chromatograph (HPLC, Waters Millipore Corp., Milford, MA, USA). The HPLC refractive index detector (Waters 2414) was set at 37 ºC. Samples were eluted from the columns at 85 ºC (connected in series Aminex HPX-87P and Aminex HPX-87C, 300 mm x 7.8 mm, BioRad) with water at 0.6 mL min^{-1} flow rate and a

total run time of 45 min. Sucrose, glucose and fructans were collected and transferred to tin capsules for isotope analysis. The use of the purification pre-columns, together with the two Aminex columns connected in series enabled the separation of sucrose, glucose and fructans, avoiding possible contamination problems raised by Richter *et al.* (2009). Furthermore, as an additional precaution, initial and final phases of peaks were discarded when collecting the peaks. As mentioned by Richter *et al.* (2009), there is no method that enables analysis of purified starch $\delta^{13}C$. Following one of the protocols described in the study conducted by Ritcher *et al.* (2009), we analysed the $\delta^{13}C$ of the HCl-hydrolysable C (HCl-C) that is mainly composed by starch. Therefore, as suggested we use the HCl-C as a reference for starch C isotopic composition. $\delta^{13}C$ of individual sugars and HCl-C was analysed by isotope ratio mass spectrometry (Delta C, Finnigan Mat, Bremen, Germany) as described by Nogués *et al.* (2008).

C isotope composition ($\delta^{13}C$) of carbohydrates, total organic matter (TOM) and air, together with C and N analyses

Flag leaf and ear samples were collected (T_0, T_1 and T_2) and dried at 60 ºC for 48 h and then ground; 1.5 mg samples were used for analyses, and 4 biological replicates were analysed for each sample. Determinations of C, $\delta^{13}C$ and N were conducted at the Serveis Cientifico-Tècnics, University of Barcelona (Barcelona, Spain) using an elemental analyser (EA1108, Series 1, Carbo Erba Instrumentazione, Milan, Italy) coupled to an isotope ratio mass spectrometer (Delta C, Finnigan, Mat., Bremen Germany) operating in continuous flow mode.

Closed system for dark respiration sampling

Flag leaves and ears were placed separately in a gas analysis chamber to collect dark-respired CO_2 and analyse $\delta^{13}C$. The chamber was connected in parallel to the sample air hose of a LI-COR 6400 (LI-COR, Lincoln, Nebraska, USA) (Aranjuelo *et al.*, 2009a). This plastic chamber (20 x 12 x 6 10^{-6} m^3), fitted with a clear plastic lid, holds two-to-four leaves (total leaf surface *ca*. 0.005 m^2). Inlet air was passed through the chamber and monitored by the LI-COR 6400. Molar fractions of CO_2 and humidity were measured with the infrared gas analyser (IRGA) of the LI-6400. The photosynthetic photon flux (PPFD) inside the chamber was maintained at 0 μmol m^{-2} s^{-1} by covering the entire system with a black blanket.

To accumulate CO_2 for the $\delta^{13}C$ analyses, respiration samples of flag leaves and ears were collected separately in the chamber described above. The gas analysis chamber was first flushed with CO_2-free air to ensure that only the CO_2 respired in the chamber was accumulated. The CO_2 concentration inside the chamber was measured by the LI-COR 6400. When the CO_2 inside reached the 300 μmol mol^{-1} concentration value, CO_2 samples were collected and analysed as described below.

For $\delta^{13}C$ measurements corresponding to each greenhouse and plant respiration (flag leaf and ear respiration), air samples were collected using 50-mL syringes (SGE International PTY LTD, Ringwood, Australia), kept in 10-mL vacutainers (BD

Vacutainers, Plymouth, UK), and then analysed by Gas Chromatography-Combustion-Isotope Ratio Mass Spectrometry (GC-C-IRMS) at the Serveis Cientifico-Tecnics of the University of Barcelona (as previously described by Nogués *et al.*, 2008). Briefly, water vapour and oxygen from gas samples were removed and the carbon dioxide, argon, and nitrogen gases were separated by a gas chromatograph (6890N, Agilent Technologies, Palo Alto, CA, USA) coupled to an isotope ratio mass spectrometer Delta^{plus} through a GC-C Combustion III interphase (ThermoFinnigan, Bremen, Germany). The column used was a 30 m x 0.32 mm i.d. GS-GASPRO (J&W Scientific Inc., Folsom, CA, USA) and the carrier gas was helium at a flow rate of 1.2 mL min^{-1}. The injection port temperature was 220 ^{o}C. The oven temperature was kept at 60 ^{o}C during the entire run. Injection was conducted in the split mode (injected volume 0.3 mL, split flow 20 mL min^{-1}).

$^{13}C/^{12}C$ ratios of air samples and plant materials were expressed in δ notation:

$$\delta^{13}C = \left(\frac{R_{sample}}{R_{standard}} \right) - 1$$

where R_{sample} refers to plant material and $R_{standard}$ to Pee Dee Belemnite (PDB) calcium carbonate.

C isotope discrimination (Δ) of leaf and ear TOM was calculated as described by Farquhar *et al.* (1989):

$$\Delta = \frac{\delta_a - \delta_p}{\delta_p + 1}$$

where δ_a and δ_p denote air ($\delta^{13}C_a$) and plant ($\delta^{13}C_p$) isotopic composition, respectively.

Proteomic characterisation

Four biological replicates of flag leaf samples (200 mg fresh weight) were ground in a mortar using liquid nitrogen and re-suspended in 2 mL of cold acetone containing 10% TCA. After centrifugation at 16,000 *g* for 3 min at 4 °C, the supernatant was discarded and the pellet was rinsed with methanol, acetone, and phenol solutions as previously described by Wang *et al*. (2003). The pellet was stored at –20 °C or immediately re-suspended in 200 µL of R2D2 rehydratation buffer (5 M urea, 2 M thiourea, 2 % 3-[(3-cholamidopropyl) dimethyl-ammonio]-1-propane-sulfonate, 2 % N-decyl-N,N-dimethyl-3-ammonio-1-propane-sulfonate, 20 mM dithiothreitol, 5 mM Tris (2-carboxyethyl) phosphine, 0.5% IPG buffer (pH 4 to 7, GE Healthcare, Saclay, France) (Mechin *et al*., 2003). The total soluble protein (TSP) concentration was determined by the method of Bradford (Bradford, 1976) using BSA as standard.

For Two-Dimensional Electrophoresis, the extract of proteins was first separated according to charge in the electrofocusing PROTEAN IEF system (Bio-Rad), at 20 °C, using 18-cm gel strips (linear pH gradient from 4 to 7, GE Healthcare). Each strip was

rehydrated at 50 µA/gel for 14h in the presence of 330 µL of R2D2 buffer containing 125 µg of proteins. Isoelectric focusing was run for 15 min at 250 V, 2 h at 500 V, and then until 50 kV at 10,000 V. After electrofocusing, the strips were equilibrated in the first buffer (75 mM Tris-HCL, 3 % (w/v) SDS, 300 mM Tris Base) containing DTT (65 mM) followed by incubation in the same buffer containing iodoacetamide (50 mM) and bromophenol (0.5 %). Second dimension electrophoresis was carried out on 12% polyacrylamide gels (20 cm × 20 cm) using an Investigator system (MILLIPORE, Saint-Quentin Fallavier, France) at 300 mV. Gels were stained using the silver staining procedure described by Blum *et al*. (1987).

After staining, the images of the two-dimensional gels were acquired with the ProXPRESS 2D proteomic Imaging System and analysed using Phoretix 2-D Expression Software v2004 (Nonlinear Dynamics, Newcastle upon Tyne, UK). Gels from four independent biological replicates were used and the analysis of gels was performed as previously described by Aranjuelo *et al.* (2010). Mr and pI were calculated using Samespots software calibrated with commercial molecular mass standards (precision protein standards prestained; Bio-Rad) run in a separate marker lane on the 2-DE gel. ANOVA ($P < 0.05$) was performed using MiniTAB to compare the relative abundance of the total volume of all detected spots for each gel.

For the protein identification by ESI-LC MS/MS, excised spots were washed several times with water and dried for a few minutes. Trypsin digestion was performed overnight with a dedicated automated system (MultiPROBE II, PerkinElmer). The gel fragments were subsequently incubated twice for 15 min in a H_2O/CH_3CN solution to allow extraction of

peptides from the gel pieces. Peptide extracts were then dried and dissolved in starting buffer for chromatographic elution, which consisted of 3 % CH_3CN and 0.1 % HCOOH in water. Peptides were enriched and separated using a lab-on-a-chip technology (Agilent, Massy, France) and fragmented using an on-line XCT mass spectrometer (Agilent). The fragmentation data were interpreted using the Data Analysis program (version 3.4, Bruker Daltonic, Billerica, USA). For protein identification, tandem mass spectrometry peak lists were extracted and compared with the protein database using the MASCOT Daemon (version 2.1.3; Matrix Science, London, UK) search engine as previously described by Desclos *et al.* (2009). Only peptides matching an individual ion score > 51 were considered. Proteins with two or more unique peptides matching the protein sequence were automatically considered as a positive identification. Among the positive matches based on one unique peptide, the fragmentation spectrum from each peptide was manually interpreted using the conventional fragmentation rules. Measured peptides were searched in the NCBInr-protein sequence database viridiplantae (green plants). Once the proteins were identified, we proceeded to their presumed biological function according to Bevan *et al.* (1998). The authors would like to clarify that apparent discrepancies concerning Rubisco concentration decreases observed by SDS-PAGE and not by the 2-DE were explained by saturation of the silver staining of Rubisco in the 2-DE methodology, due to its abundance.

Statistical analyses

Data was processed by one-factor analysis of variance (ANOVA). Means ± standard errors (SE) were calculated, and when the *F*-ratio was significant, least significant differences were evaluated by the LSD test using the statistical software package SPSS 12.0 (SPSS

Inc., Chicago, IL, USA). The results were accepted as significant at $P < 0.05$. All values shown in the figures and tables are means ± SE.

Results

Growth in elevated [CO_2] had no effect on leaf and total biomass; however, ear DM marginally decreased (P= 0.093) in these treatments (Table 1). Furthermore, no significant differences were observed in ear DM / total DM ratio. At the respective growth CO_2 conditions, flag leaf photosynthesis was higher in elevated than ambient CO_2 plants, although the difference did not reach significance (Table 1). However, when photosynthesis was determined at a common concentration of 370 or 700 μmol m^{-2} s^{-1} (A_{370} and A_{700} respectively) the results revealed that plants grown under elevated [CO_2] had lower photosynthetic rates. Intercellular [CO_2] (C_i) and stomatal conductance values (g_s) determined at the same [CO_2] (g_{350} *versus* g_{700} and Ci_{370} *versus* Ci_{700} respectively), showed that limitations in C_i were not the cause of the lower photosynthetic capacity of plants exposed to elevated [CO_2] (Table 1).

The leaf carbohydrate determinations (Fig. 1) showed that although glucose and sucrose were not affected by [CO_2], starch (marginally) and fructan concentration increased in plants exposed to 700 μmol mol^{-1}. In ears, no significant differences were detected in any of the analysed carbohydrates. As shown in Figure 2, N content decreased in leaves exposed to elevated [CO_2], whereas no significant differences were detected in ears. The C/N ratio showed an increase in flag leaves and no significant difference in ears in response

to elevated [CO_2]. Figure 3 shows that leaf N, Rubisco and amino acid content decreased in elevated [CO_2]. Although total soluble protein (TSP) content was not significantly affected by [CO_2], the percentage of Rubisco in TSP decreased in elevated [CO_2]. Total Rubisco activity (Fig.4) was decreased by elevated [CO_2] while initial Rubisco activity was not significantly affected, because Rubisco activation increased. The k_{cat} of Rubisco (Fig. 4) was significantly lower in elevated than ambient [CO_2].

During post-anthesis and after 7 days of labelling, the $\delta^{13}C$ in leaf total organic matter (TOM) was -39.92 ‰ and this value was constant for 24 and 48 hours (-40.22 and -40.08 ‰ respectively) after the end of labelling (Fig. 5). Interestingly, the analyses of leaf respired CO_2 also revealed that in elevated [CO_2], the (T_0) $\delta^{13}C$ was lower in labelled than non-labelled plants (-34.10 and -30.72 ‰ respectively) immediately after the labelling. However such depletion decreased to -32.36 ‰ by 24 hours and to -31.12 ‰ by 48 hours after the end of labelling (Fig. 5). For ears of labelled and non-labelled plants in elevated [CO_2], the similar $\delta^{13}C$ in TOM (-36.90 and -37.75 ‰, respectively) and in respired CO_2 (-33.51 and -33.66 ‰, respectively) suggests that no labelled C was present in ears (Fig. 5). In both flag leaves and ears, the sucrose and fructans $\delta^{13}C$ was similar in labelled and non-labelled plants exposed to 700 μmol mol^{-1} (Fig. 5). However, for leaf glucose immediately after the end of labelling (T_0), $\delta^{13}C$ changed from -33.43 ‰ in non labelled plants to -35.97 ‰ in labelled plants. Twenty-four (T_1) and 48 (T_2) hours later, the corresponding $\delta^{13}C$ values were -35.49 ‰ and -30.98 ‰ (Fig. 5). In ears exposed to elevated [CO_2], the $\delta^{13}C$ of glucose immediately after labelling was similar in labelled and non labelled plants (-32.37 and -31.69 ‰, respectively). As shown in Fig. 5, such values were depleted to -34.03 ‰ at

T1 and to -31.66 ‰ at T2. Figure 5 also shows that $\delta^{13}C$ of leaf starch in elevated [CO_2] conditions was -38.01 ‰ in labelled plants and -35.81 ‰ in non-labelled plants. Such values were maintained at T_1 and T_2. However, Fig. 5 also shows that starch in ears of labelled (-34.93 ‰) and non labelled (-34.20 ‰) plants had a similar $\delta^{13}C$.

The elevated CO_2 effect on the leaf protein pattern in wheat plants was studied using 2-DE (Fig. 6). Our protocol enabled the identification of 14 proteins that differed in their expression under ambient and elevated CO_2 conditions (Tables 2 and 3). Eight of these proteins were up-regulated under elevated CO_2 conditions (Table 2), with the remaining 6 being down-regulated (Table 3). These proteins were classified in different groups according to their presumed biological function. The up-regulated proteins were classified into 6 groups: metabolism processes (1 protein identified), energy processes (1 protein identified), transporters (1 protein identified), disease/defence processes (1 protein identified), proteins with unclear classification (2 proteins identified) and unclassified proteins (2 proteins identified). Among the down-regulated proteins, energy processes (2 proteins identified), disease/defence (1 protein identified) and unclassified proteins (3 proteins identified) were detected. The roles of these proteins are discussed in the following section with regard to the changes in physiological traits in response to elevated CO_2 conditions.

Discussion

A review of wheat performance under elevated [CO_2] in 156 experiments (Amthor, 2001) has shown CO_2 responses ranging from no effect or a negative one in some studies to

several-fold increases in others. As shown in Table 1, the fact that exposure to 700 μmol mol^{-1} CO_2 marginally decreased ear DM during the post-anthesis period (P= 0.093) and that no effect was observed in total DM and ear DM / total DM, revealed that in agreement with Högy *et al.* (2009), elevated [CO_2] did not contribute to increased grain filling (Amthor, 2001; Uddling *et al.*, 2008). Our results were corroborated in the supplementary harvest conducted at the grain maturity stage (see supplementary Table). Absence of effects on total DM, together with the lower ear DM suggest that under elevated [CO_2] exposure, the plants invested a larger amount of photoassimilates in the development of vegetative biomass rather than in grain filling. Grain filling may be limited by (i) translocation of photoassimilates from source to sink, (ii) photosynthetic activity and (iii) ear sink capacity (Uddling *et al.*, 2008). Evans *et al.* (1970) showed that assimilate movement from leaves to ears in wheat was not limited by phloem stem transport. Photosynthesis (measured at the respective growth conditions) was increased only to a limited extent by elevated [CO_2] (Table 1). Moreover, when photosynthetic activity was determined in all plant treatments at 370 and 700 μmol mol^{-1} [CO_2] (Table 1) it was found that plants grown in elevated [CO_2] had lower photosynthetic capacity than plants grown in ambient [CO_2] (Zhang *et al.*, 2009). Photosynthetic acclimation has been previously described in wheat plants exposed to elevated [CO_2] in greenhouses located in the field (Martínez-Carrasco *et al.*, 2005; Alonso *et al.*, 2009; Gutiérrez *et al.*, 2009). Although exposure to elevated [CO_2] decreased stomatal conductance (*gs*), similar (Ci_{700}) or even higher (Ci_{370}) intercellular CO_2 concentrations (C_i) in elevated [CO_2] than ambient [CO_2] ruled out stomatal closure as the main cause of the reduction in photosynthetic capacity in elevated [CO_2]. Carbonic anhydrase (CA), a protein that catalyses the reversible conversion of CO_2 to HCO_3^-, has

been recognised as an important enzyme that is closely associated with photosynthesis (Sasaki *et al.*, 1998). We have found a 198% increase in this enzyme in elevated [CO_2] relative to control leaves that could partly compensate for the closure of stomata and ensure the supply of CO_2 to the chloroplasts.

The SDS-PAGE densitometric analysis revealed that the photosynthetic down-regulation in elevated [CO_2] was caused by a lower Rubisco protein content (Fig. 3) (Theobald *et al.*, 1998; Aranjuelo *et al.*, 2005a). This decrease was not detected by the proteomic analysis due to the saturation of the silver staining used in the latter. Moreover, the proteomic characterisation showed a decrease in Rubisco activase content in plants exposed to 700 μmol mol^{-1} CO_2 (Table 3). Rubisco activase is essential for the maintenance of Rubisco catalytic activity by promoting the removal of tightly bound inhibitors from the catalytic sites (Robinson and Portis, 1989; Parry *et al.*, 2008). The lower photosynthetic rates of plants exposed to 700 μmol mol^{-1} [CO_2] (Table 3) may be a consequence both of decreased Rubisco protein and increased binding of inhibitors to Rubisco active sites, which is consistent with the decreased k_{cat} of the enzyme in elevated [CO_2] found in this (Fig. 4) and previous studies (Pérez *et al.*, 2005; 2007).

Lack of significant differences in total soluble protein (TSP) content, and the decrease of Rubisco as a fraction of TSP (Fig. 3) revealed that the diminished Rubisco concentration was caused by a specific inhibition of this protein in leaves exposed to elevated [CO_2] (Pérez *et al.*, 2007). According to Zhu *et al.* (2009) and Fangmeier *et al.* (2000), in flag leaves of wheat exposed to elevated [CO_2] there is an increase in protease activity that

enables the remobilisation of N. In agreement with this finding, the lower amino acid level in flag leaves (Table 2) under elevated [CO_2] suggests that the flag leaf Rubisco-derived N was reallocated to the ear, an organ with high N sink capacity. Furthermore, according to Theobald *et al.* (1998), in elevated [CO_2] there is a greater reduction in Rubisco than in other photosynthetic components (ATP synthase, etc.). The up-regulation of proteins involved in RuBP regeneration, like ATP synthase (β subunit), ruled out limitations on RuBP regeneration as the cause of diminished carboxylation in elevated [CO_2], and suggests a rebalancing away from carboxylation to RuBP-regeneration capacity (Theobald *et al.*, 1998).

The decrease in photosynthetic capacity under elevated [CO_2] has been attributed to end product inhibition, in which the demand for carbohydrates is insufficient to cope with the enhanced carbohydrate supply (Rogers and Ellsworth, 2002; Ainsworth and Long, 2005; Aranjuelo *et al.*, 2008). The accumulation of fructans and starch in flag leaves in elevated CO_2 (Fig. 1) was associated with decreases of Rubisco (Fig. 2) and Rubisco activase (Table 3) proteins, and may be causal in down-regulation of photosynthetic capacity (Moore *et al.*, 1999; Jifon and Wolfe, 2002). As shown in Tables 2 and 3, the proteomic characterisation provided relevant information concerning the possible involvement of altered protein levels in carbon metabolism in elevated CO_2. Our study revealed that phosphoglycerate mutase (PGAM) content increased by 627.13 % in plants grown in elevated [CO_2] (Table 2). PGAM catalyses the intercoversion of 3-phosphoglycerate (3-PGA) to 2-phosphoglycerate (2-PGA) (Batz *et al.*, 1992), and its increase could lead to enhanced glycolysis. Carbohydrate accumulation in leaves,

irrespective of whether it is a result of sugar-feeding or an inhibition of phloem transport or growth in elevated [CO_2], has been shown to stimulate organic acid synthesis (Morcuende *et al.*, 1998; Stitt and Krapp, 1999) and respiratory pathways, leading to a decrease in the levels of 3-PGA (Morcuende *et al.*, 1996; Morcuende *et al.*, 1997) and increased formation of ATP (Stitt and Krapp, 1999). Furthermore, the proteomic characterisation also revealed a 79% decrease of adenosine diphosphate glucose pyrophosphatase (AGPPase) in elevated [CO_2] (Table 3). AGPPase catalyses the hydrolytic conversion of ADPglucose (ADPG), the universal glucosyl donor for starch biosynthesis, to AMP and G1P (Rodriguez-López *et al.*, 2000). Although starch and fructan accumulation in leaves in elevated [CO_2] may be accounted for by the observed decrease in leaf nitrogen content, since nitrate is known to repress AGP pyrophosphorylase (Scheible *et al.*, 1997) and at least one enzyme of fructan synthesis (Morcuende *et al.*, 2004), the decrease in AGPPase protein can contribute to the observed starch build-up in elevated [CO_2]. The fact that this protein is inhibited by ATP content (Emes *et al.*, 2003), and that the ATP synthase β subunit increased under elevated [CO_2], points to a tight control of starch build-up in leaves. The up-regulation of PGAM and down-regulation of AGPPase show an altered protein pattern that can enhance C utilisation for storage and energy in elevated [CO_2].

Carbohydrate build-up in leaves is determined by the plant's ability to develop new sinks (e.g. new vegetative or reproductive structures, enhanced respiratory rates), or to expand the storage capacity or growth rate of existing sinks (Lewis *et al.*, 2002). Although respiration processes require an investment of a large quantity of photoassimilates (Amthor, 2001; Aranjuelo *et al.*, 2009b), little attention has been given to this topic (especially in

ears) in C balance studies analysing grain filling in cereals. Leaf respired $\delta^{13}C$ (Fig. 5) was depleted immediately after the $^{12}CO_2$ labelling and 24 h (T_1) and 48 h (T_2) later, showing that these plants were respiring, in part, C assimilated during the labelling period. However the fact that 48 h later (T_2) the $\delta^{13}C$ was similar to the values obtained before labelling (E) suggests that two days after labelling the leaves had respired almost all the labelled respiratory substrates. The determination of $\delta^{13}C$ in the various carbohydrates (Fig. 5), suggested that these leaves were respiring the labelled total soluble sugar (TSS) and especially glucose. This point is reinforced by the fact that 48 h after the end of labelling, no labelled C was present among glucose C, which is similar to the observation for leaf respiration $\delta^{13}C$. Opposite to the observation for leaf respiration and soluble sugar, the $\delta^{13}C$ of total organic matter (TOM) of flag leaves remained constant even 48 hours after the end of labelling. Such results could be explained by the fact that part of the labelled C was partitioned to structural and storage compounds. While fructan $\delta^{13}C$ did not contribute detectable labelled C in flag leaves, the $\delta^{13}C$ depletion in starch (-35.81 ‰ in non-labelled plants *versus* -37.93 ‰ in labelled plants) revealed that part of the labelled C present in TOM was accounted for by C accumulation in starch. It is very likely that because no labelled C was present in soluble sugars 48 h after the labelling, most of the remaining labelled C consisted of structural C compounds. The fact that TOM was more depleted than starch (-39.86 and -37.93 ‰ respectively) confirmed this point.

As mentioned above, leaf carbohydrate in wheat is also determined by ear C sink strength. Our data revealed that although exposure to 700 μmol mol^{-1} CO_2 did not modify sucrose and glucose concentrations in ears, fructan and starch concentrations tended to

increase. During grain filling, the strong C demand by wheat ears is met with ear photosynthesis and respiration (Tambussi *et al.*, 2007), together with translocation of C from flag leaves and stem internodes (Gebbing *et al.*, 1999; Aranjuelo *et al.*, 2009b). Absence of differences in the $\delta^{13}C$ in ear TOM and respired CO_2 between labelled and non-labelled plants (Fig. 5) confirmed that exposure to elevated [CO_2] did not increase ear filling during the beginning of anthesis, which is in agreement with the data on ear DM/ total DM ratios (Table 1). Even if the ear TOM was not labelled, the fact that sucrose and glucose $\delta^{13}C$ was depleted (Fig. 5) highlighted that a small fraction of labelled C reached the ear. Apparent discrepancies in TOM and sugar $\delta^{13}C$ could be explained by the fact that glucose and sucrose concentrations represent a small fraction of ear C and therefore labelled C was diluted in TOM that was almost totally composed by non-labelled C (see Fig. 2). Although the photosynthetic activity of ears should not be ignored (Tambussi *et al.*, 2007; Zhu *et al.*, 2009), the fact that glucose, total soluble sugar and especially sucrose $\delta^{13}C$ depletion was more marked 24 and 48 hours after the labelling, indicates that this labelled C originated in flag leaves.

In summary this study suggested that the absence of elevated [CO_2] effects on biomass production, and especially ear grain filling, reflected the inability of these wheat plants to increase C sink strength. Absence of elevated [CO_2] effects on biomass production of plants with larger photosynthetic rates caused a leaf carbohydrate build-up. Such an increase induced photosynthetic acclimation, as reflected by the lower carboxylation capacity of treatments exposed to 700 μmol mol^{-1}. The isotopic characterisation conducted during the post-anthesis period showed that, in flag leaves, part of the newly assimilated C

was allocated to storage compounds and that another part of labelled C (mainly soluble sugars) was totally respired 48 h after the end of labelling. Interestingly, in ears, $\delta^{13}C$ data revealed that although no labelled C was detected in ear total organic matter (TOM), a small amount of C reached the ears in the form of soluble sugars. Proteomic characterisation showed that in these plants the changes in protein content enhanced C storage and glycolysis. Furthermore, the protein characterisation also revealed that photosynthetic acclimation was caused by a decrease in Rubisco protein content and in the capacity to release Rubisco tight-binding inhibitors. The decreases in leaf N, Rubisco and amino acid content suggest that under elevated [CO_2] there was a reallocation of leaf N to ears during grain filling.

Acknowledgements

The technical cooperation of AL Verdejo and MA Boyero in gas exchange and growth measurements, and in analyses of Rubisco protein, amino acids and total nitrogen content is acknowledged. We thank the staff of Muñovela experimental farm for technical assistance in crop husbandry. The assistance of Pilar Teixidor during the isotopic analyse is greatly acknowledged. This work has been funded by the Spanish National Research and Development Programme-European Regional Development Fund ERDF (Projects AGL2006-13541-C02-01/ AGL2006-13541-C02-02 and CGL2009-13079-C02-02).

References

Ainsworth EA, Long SP. 2005 What have we learned from 15 years of free-air CO_2 enrichment (FACE)? A meta-analytic review of responses of photosynthesis, canopy properties and plant production to rising CO_2. *New Phytologyst* **165**, 351-372.

Alonso A, Pérez P, Martínez-Carrasco R. 2009. Growth in elevated CO_2 enhances temperature response of photosynthesis in wheat. *Physiologia Plantarum* **135**, 109–120.

Amthor JS. 2001. Effects of atmospheric CO_2 concentration on wheat yield: review or results from experiments using various approaches to control CO_2 concentration. *Field Crop Research* **73**, 1-34.

Aranjuelo I, Zita G, Hernandez L, Pérez P, Martínez-Carrasco R, Sánchez-Díaz M. 2005a. Response of nodulated alfalfa to water supply, temperature and elevated CO_2: Photosynthetic down-regulation. *Physiologia Plantarum* **123**, 348-358.

Aranjuelo I, Irigoyen JJ, Pérez P, Martínez-Carrasco R, Sánchez-Díaz M. 2005b. The use of temperature gradient greenhouses for studying the combined effect of CO2, temperature and water availability in N_2 fixing alfalfa plants. *Annals of Applied Biology* **146**, 51–60.

AranjueloI, Irigoyen JJ, Sánchez-Díaz M, Nogués S. 2008. Carbon partitioning in N_2 fixing Medicago sativa plants exposed to different CO_2 and temperature conditions. *Functional Plant Biology* **35**, 306-317.

Aranjuelo I, Pardo T, Biel C, Savé R, Azcón-Bieto J, Nogués S. 2009a. Leaf carbon management in slow-growing plants exposed to elevated CO_2. *Global Change Biology* **15**, 97-109.

Aranjuelo I, Cabrera-Bosquet Ll, Mottaleb SA, Araus JL, Nogués S. 2009b. $^{13}C/^{12}C$ isotope labeling to study carbon partitioning and dark respiration in cereals subjected to water stress. *Rapid Communication in Mass Spectrometry* **23**, 2819-2828.

Aranjuelo I, Molero G, Erice G, Avice JC, Nogués S. 2010. Plant physiology and proteomics reveals the leaf response to drought in alfalfa (*Medicago sativa* L.). *Journal of Experimental Botany* (In press).

Araus JL, Brown HR, Febrero A, Bort J, Serret MD. 1993. Ear photosynthesis, carbon isotope discrimination and the contribution of respiratory CO_2 to differences in grain mass in durum wheat. *Plant Cell and Environment* **16**, 383-392.

Batz O, Scheibe R, Neuhaus EH. 1992. Transport Processes and Corresponding Changes in Metabolite Levels in Relation to Starch Synthesis in Barley (*Hordeum vulgare* L.) Etioplasts. *Plant Physiology* **100**, 184-190.

Bevan M, Bancroft I, Bent E, et al. 1998. Analysis of 19 Mb of ontiguous sequence from chromosome 4 of Arabidopsis thaliana. *Nature* **391**, 485–488.

Blum H, Beier H, Gross HJ. 1987. Improved silver staining of plant proteins, RNA and DNA in polyacrylamid gel. *Electrophoresis* **8**, 93–99

Bort J, Brown HR, Araus JL. 1996. Refixation of respiratory CO_2 in the ears of C_3 cereals. *Journal of Experimental Botany* **47**, 1567–1575.

Bradford MM. 1976. A rapid method for the quantification of microgram quantities of protein utilizing the principle of protein-dye binding. *Annals of Biochemistry* **72**, 248–254.

Farquhar GD, von Caemmerer S, Berry JA. (1980) A biochemical model of photosynthetic CO_2 assimilation in leaves of C_3 species. *Planta* **149**, 78–90.

Desclos M, Etienne P, Coquet L, Cosette P, Bonnefoy J, Segura R, Reze S, Ourry A, Avice JC. 2009. A combined ^{15}N tracing/proteomics study in Brassica napus reveals the chronology of proteomics events associated to N remobilisation during leaf senescence induced by nitrate limitation or starvation. *Proteomics* **9**, 3580–3608.

Davey PA, Hunt S, Hymus GJ, DeLucia EH, Drake BG, Karnosky DF, Long SP. 2004. Respiratory oxygen uptake is not decreased by an instantaneous elevation of [CO_2], but is increased with long-term growth in the field at elevated [CO_2]. *Plant Physiology* **134**, 1-8.

Davey PA, Olcer H, Zakhleniuk O, Bernacchi CJ, Calfapietra C, Long SP, Raines CA. 2006. Can fast-growing plantation trees escape iochemical downregulation of photosynthesis when grown throughout their complete production cycle in the open air under elevated carbon dioxide? *Plant, Cell and Environment* **29**, 1235-1244.

Ellsworth DS, Reich PB, Naumburg ES, Koch GW, Kubiske ME, Smith SD. 2004. Photosynthesis, carboxylation and leaf nitrogen responses of 16 species to elevated pCO_2 across four free-air CO_2 enrichment experiments in forest, grassland and desert. *Global Change Biology* **10**, 2121-2138.

Emes MJ, Bowsher CG, Hedley C, Burrell MM, Scrase-Field ESF, Tetlow IJ. 2003. Starch synthesis and carbon partitioning in developing Endosperm. *Journal of Experimental Botany* **54**, 569-575.

Evans L T, Dunstone RL, Rawson HM., Williams RF. 1970. Phloem of wheat stem in relation to requirements for assimilate by ear. *Australian Journal of Biological Sciences* **23**, 743-752.

Evans LT,Wardlaw IF, Fischer RA. 1975. Wheat. In Evans LT, ed. Crop Physiology;Some Case of Histories. Cambridge University Press, Cambridge, UK, pp.101–150.

Fangmeier A, Chrost B, Hogy P. Krupiskam K. 2000. CO_2 enrichment enhances flag senescence in barley due to greater grain nitrogen sink capacity. *Environmental and Experimental Botany* **44**, 151-164.

Farquhar GD, Hubick KT, Condon AG, Richards RA. 1989. Carbon isotope fractionation and water-use efficiency. In Rundel PW, Ehleringer JR, Nagy KA, eds. Stable isotopes in ecological research, vol. 68, Ecological Studies. Springer-Verlag, Berlin, Germany, pp 21-40.

von Felten S, Hättenschwiler S, Saurer M, Siegwolf R. 2007. Carbon allocation in shoots of alpine treeline conifers in a CO_2 enriched environment. *Trees* **21**, 283-294.

Gebbing T, Schnyder H. 1999. Pre-anthesis reserve utilization for protein and carbohydrate synthesis in grains of wheat. *Plant Physiology* **121**, 871–878.

Gutiérrez D, Gutiérrez E, Pérez P, Morcuende R, Verdejo AL, Martínez-Carrasco R. 2009. Acclimation to future atmospheric CO_2 levels increases photochemical efficiency and mitigates photochemistry inhibition by warm temperatures in wheat under field chambers. *Physiologia plantarum* **137**, 86-100.

Hare PE. 1977. Subanomale range amino acid analyses. *Methods in enzymology* **43**, 3-18.

Högy P, Zörb C, Langenkämper G, Betsche T, Fangmeier A. 2009. Atmospheric CO_2 enrichment changes the wheat grain proteome. *Journal of Cereal Science* **50**, 248-254.

Jifon JL, Wolfe DW. 2002. Photosynthetic acclimation to elevated CO_2 in *Phaseolus vulgaris* L. is altered by growth response to nitrogen supply. *Global Change Biology* **8**, 1018–1027.

Kodama N, Ferrio JP, Brüggemann, Gessler A. 2010. Short-term dynamics of the carbon isotope composition of CO_2 emitted from a wheat agroecosystem – physiological and environmental controls. *Plant Biology* doi:10.1111/j.1438-8677.2010.00329.x

Körner C, Asshoff R, Bignucolo O, Hättenschwiler S, Keel SG, Peláez-Riedl S, Pepin S, Siegwolf RTW, Zotz G. 2005. Carbon Flux and Growth in Mature Deciduous Forest Trees Exposed to Elevated CO_2. *Science* **309**, 1360-1362.

Lewis JD, Wang XZ, Griffin KL, Tissue DT. 2002. Effects of age and ontogeny on photosynthetic responses of a determinate annual plant to elevated CO_2 concentrations. *Plant, Cell and Environment* **25**, 359–368.

Long SP, Ainsworth EA, Rogers A, Ort DR 2004. Rising atmospheric carbon dioxide: Plants FACE the future. *Annual Review of Plant Biology* **55**, 591-628.

Martínez-Carrasco R, Pérez P, Morcuende R. 2005. Interactive effects of elevated CO_2, temperature and nitrogen on photosynthesis of wheat grown under temperature gradient tunnels. *Environmental and Experimental Botany* **54**, 49–59.

Mechin V, Consoli L, Le Guilloux M, Damerval C. 2003. An efficient solubilization buffer for plant proteins focused in immobilized pH gradients. *Proteomics* **3**, 1299–1302.

Moore BD, Cheng SH, Sims D, Seemann JR. 1999. The biochemical and molecular basis for photosynthetic acclimation to elevated atmospheric CO_2. *Plant, Cell and Environment* **22**, 567-582.

Morcuende R, Pérez P, Martínez-Carrasco R, Martín del Molino I, Sánchez de la Puente L. 1996. Long- and short-term responses of leaf carbohydrate levels and photosynthesis to decreased sink demand in soybean. *Plant, Cell and Environment* **19**, 976-82.

Morcuende R, Pérez P, Martínez-Carrasco R. 1997. Short-term feedback inhibition of photosynthesis in wheat leaves supplied with sucrose and glycerol at two temperatures. *Photosynthetica* **33**, 179-188.

Morcuende R, Krapp A, Hurry V, Stitt M. 1998. Sucrose feeding leads to increased rates of nitrate assimilation, increased rates of oxoglutarate synthesis, and increased rates of a wide spectrum of amino acids in tobacco leaves. *Planta* **26**, 394-409.

Morcuende R, Kostadinova S, Pérez P, Martín del Molino IM, Martínez-Carrasco R. 2004. Nitrate is a negative signal for fructan synthesis, and the fructosyltranferase-inducing trehalose inhibits nitrogen and carbon assimilation in excised barley leaves. *New Phytologist* **161**, 749-759.

Nakano H, Makino A, Mae T. 1997. The effect of elevated partial pressures of CO_2 on the relationship between photosynthetic capacity and N content in rice leaves. *Plant Physiology* **115**, 191-198.

Naumburg E, Housman DC, Huxman T, Charlet TN, Loik ME, Smith SD. 2004. Photosynthetic responses of Mojave Desert shrubs to free-air CO_2 enrichment are greatest during wet years. *Global Change Biology* **8**, 276-285.

Nogués S, Tcherkez G, Cornic G, Ghashghaie J. 2004. Respiratory carbon metabolism following illumination in intact French bean leaves using $^{13}C/^{12}C$ isotope labeling. *Plant Physiology* **136**, 3245-3254.

Nogués S, Aranjuelo I, Pardo T, Azcón-Bieto J. 2008. Assessing the stable-carbon isotopic composition of intercellular CO_2 in a CAM plant at two CO_2 levels. *Rapid Communications in Mass Spectrometry* **22**, 1017-1022.

Nowak RS, Ellsworth DS, Smith SD. 2004. Functional responses to elevated atmospheric CO_2 – do photosynthetic and productivity data from FACE experiments support early predictions? *New Phytologist* **162**, 253-280.

Parry MAJ, Keys AJ, Madgwick PJ, Carmo-Silva AE, Andralojc PJ. 2008. Rubisco regulation: a role for inhibitors. *Journal of Experimental Botany* **59**, 1569-1580.

Pérez P, Morcuende R, Martín del Molino I, Martínez-Carrasco R. 2005. Diurnal changes of Rubisco in response to elevated CO_2, temperature and nitrogen in wheat grown under temperature gradient tunnels. *Environmental and Experimental Botany* **53**, 13–27.

Pérez P, Zita G, Morcuende R, Martínez-Carrasco R. 2007. Elevated CO_2 and temperature differentially affect photosynthesis and resource allocation in flag and penultimate leaves of wheat. *Photosynthetica* **45**, 9–17

Prentice IC, Farquhar GD, Fasham MJR, et al. 2001. The carbon cycle and atmospheric carbon dioxide. In Houghton JT, Ding Y, Griggs DJ, Noguer M, van der Linden PJ, Xiaosu D eds. Climate change 2001: the scientific basis. Contribution of Working Group I to the Third Assessment Report of the Intergovernmental Panel on Climate Change. New York: Cambridge University Press, USA, pp183-239.

Rawson HM, Gifford RM, Condon BN. 1995. Temperature gradient chambers for research on global environment change. Part I. Portable chambers for research on short-stature vegetation. *Plant Cell and Environment* **18**, 1048–1054.

Robinson SP, Portis AR. 1989. Adenosine triphosphate hydrolysis by purified Rubisco activase. *Archives of Biochemistry and Biophysics* **268**, 93-99.

Rodríguez-López M, Baroja-Fernández E, Zandueta-Criado A, Pozueta-Romero J. 2000. Adenosine diphosphate glucose pyrophosphatase: A plastidial phosphodiesterase that prevents starch biosynthesis. *Proceedings of the Natural Academy Science* **97**, 8705-8710.

Rogers A, Ellsworth DS. 2002. Photosynthetic acclimation of *Pinus taeda* (loblolly pine) to long-term growth in elevated *p*CO2 (FACE). *Plant, Cell and Environment* **25**, 851–858.

Richter A, Wanek W, Werner RA, Ghashghaie J, Jäggi M, Gessler A, Brugnoli E, Hettmann E, Göttlicher SG, Salmon Y, Bathellier C, Kodama N, Nogués S, SØe A, Volders F, Sörgel K, Blöchl A, Siegwolf RTW, Buchmann N, Gleixner G. 2009. Preparation of starch and soluble sugars of plant material for the analyses of carbon isotope composition: a comparison of methods. *Rapid Communication in Mass Spectrometry* **23**, 2476-2488.

Sasaki H, Hirose T, Watanabe Y, Ohsugi R. 1998. Carbonic Anhydrase Activity and CO_2-Transfer Resistance in Zn-Deficient Rice Leaves. *Plant Physiology* **118**, 929–934.

Scheible WR, González-Fontes A, Lauerer M, Müller-Rober B, Caboche M, Stitt M. 1997. Nitrate acts as a signal to induce organic acid metabolism and repress starch metabolism in tobacco. *The Plant Cell* **9**, 783-798.

Schnyder H. 1993. The role of carbohydrate storage and redistribution in the source-sink relations of wheat and barley during grain filling – a review. *New Phytologist* **123**, 233-245.

Schnyder H, Schäufele R, Lötscher M, Gebbing T. 2003. Disentangling CO_2 fluxes: direct measurements of mesocosm-scale natural abundance $^{13}CO_2$ / $^{12}CO_2$ gas exchange, ^{13}C discrimination, and labelling of CO_2 exchange flux components in controlled environments. *Plant, Cell and Environment* **26**, 1863–1874.

Stitt M, Krapp A. 1999. The interaction between elevated carbon dioxide and nitrogen nutrition: the physiological and molecular background. *Plant, Cell and Environment* **22**, 583–621.

Tambussi EA, Bort J, Guiamet JJ, Nogués S, Araus JL. 2007. The Photosynthetic Role of Ears in C_3 Cereals: Metabolism, Water Use Efficiency and Contribution to Grain Yield. *Critical Reviews in Plant Sciences* **26**, 1–16.

Theobald JC, Mitchell RAC, Parry MAJ, Lawlor DW. 1998. Estimating the excess investment in ribulose-1,5-bisphosphate carboxylase/oxygenase in leaves of spring wheat grown under elevated CO_2. *Plant Physiology* **118**, 945-955.

Thomas RB, Strain BR. 1991. Root restriction as a factor in photosynthetic acclimation of cotton seedlings grown in elevated carbon dioxide. *Plant Physiology* **96**, 627-634.

Uddling J, Gelang-Alfredsson J, Karlsson PE, Selldén G, Pleijel H. 2008. Source–sink balance of wheat determines responsiveness of grain production to increased [CO_2] and water supply. *Agriculture, Ecosystems and Environment* **127**, 215–222.

Wang W, Scali M, Vignani R, Spadafora A, Sensi E, Mazzuca S, Cresto M. 2003. Protein extraction for two-dimensional electrophoresis from olive leaf, a plant tissue containing high levels of interfering compounds. *Electrophoresis* **24**, 2369–2375.

Zhang DY, Chen GY, Chen J, Yong ZH, Zhy JG, Xu DQ. 2009. Photosynthetic acclimation to CO_2 enrichment related to ribulose-1,5-bisphosphate carboxylation limitation in wheat. *Photosynthetica* **47**, 152-154.

Zhu C, Zhu J, Zeng Q, Liu G, Xie Z, Tang H, Cao J, Zhao X. 2009. Elevated CO_2 accelerates flag senescence in wheat due to ear photosynthesis which causes greater ear nitrogen sink capacity and ear carbon sink limitation. *Functional, Plant Biology* **36**, 291-299.

Figure Legends

Figure 1. Elevated [CO_2] effect on wheat flag leaf and ear glucose, sucrose, fructan and starch content 14 days after anthesis. Open bars correspond to plants grown under ambient CO_2 (ca. 370 µmol mol^{-1}) and closed bars to those grown under elevated CO_2 (ca. 700 µmol mol^{-1}). Each value represents the mean ± SE (n= 4). The different symbols indicate non significant differences (ns), significant differences $P<0.05$ (*) and $P<0.01$ (**) between treatments as determined by LSD.

Figure 2. Elevated [CO_2] effect on wheat flag leaf and ear N content and C/N ratio 14 days after anthesis. Open bars correspond to plants grown under ambient CO_2 (ca. 370 µmol mol^{-1}) and closed bars to those grown under elevated CO_2 (ca. 700 µmol mol^{-1}). Otherwise as in Figure 1.

Figure 3. Elevated [CO_2] effect on wheat flag leaf N, total soluble protein (TSP), Rubisco and amino acid content and Rubisco as a percentage of TSP 14 days after anthesis. Otherwise as in Figure 1.

Figure 4. Elevated [CO_2] effect on wheat flag leaf total Rubisco activity, Rubisco activation and Rubisco k_{cat} 14 days after anthesis. Open bars correspond to plants grown under ambient CO_2 (ca. 370 µmol mol^{-1}) and closed bars to those grown under elevated CO_2 (ca. 700 µmol mol^{-1}). Otherwise as in Figure 1.

Figure 5. Elevated [CO_2] effect on wheat flag leaf and ear ^{13}C isotopic composition ($\delta^{13}C$) in total organic matter (TOM), respired CO_2, (DR CO_2), total soluble sugars

(TSS), glucose (Glu), sucrose (suc), fructans (Fru) and starch (HCl-C). T_0, refers to the end of labelling (14 days after anthesis), whereas T_1, T_2, refer to 24 h and 48 h after the end of labelling, respectively**.** Otherwise as in Figure 1.

Figure 6. Silver-stained two-dimensional gel electrophoresis of proteins extracted from wheat leaves grown under ambient and elevated conditions 14 days after anthesis. In the first dimension, 125 mg of total protein was loaded on a 18 cm IEF strip with a linear gradient of pH 4–7. The second dimension was conducted in 12% polyacrylamide (w/v) gels (20 × 20 cm) (for details see ‘‘Materials and Methods’’). The gel image analyses was conducted with Progenesis SameSpots software v3.0 and the subsequent mass spectrometry analyses identified up to 14 proteins (marked by arrows) with significantly different expression in elevated [CO_2].

Figure 1

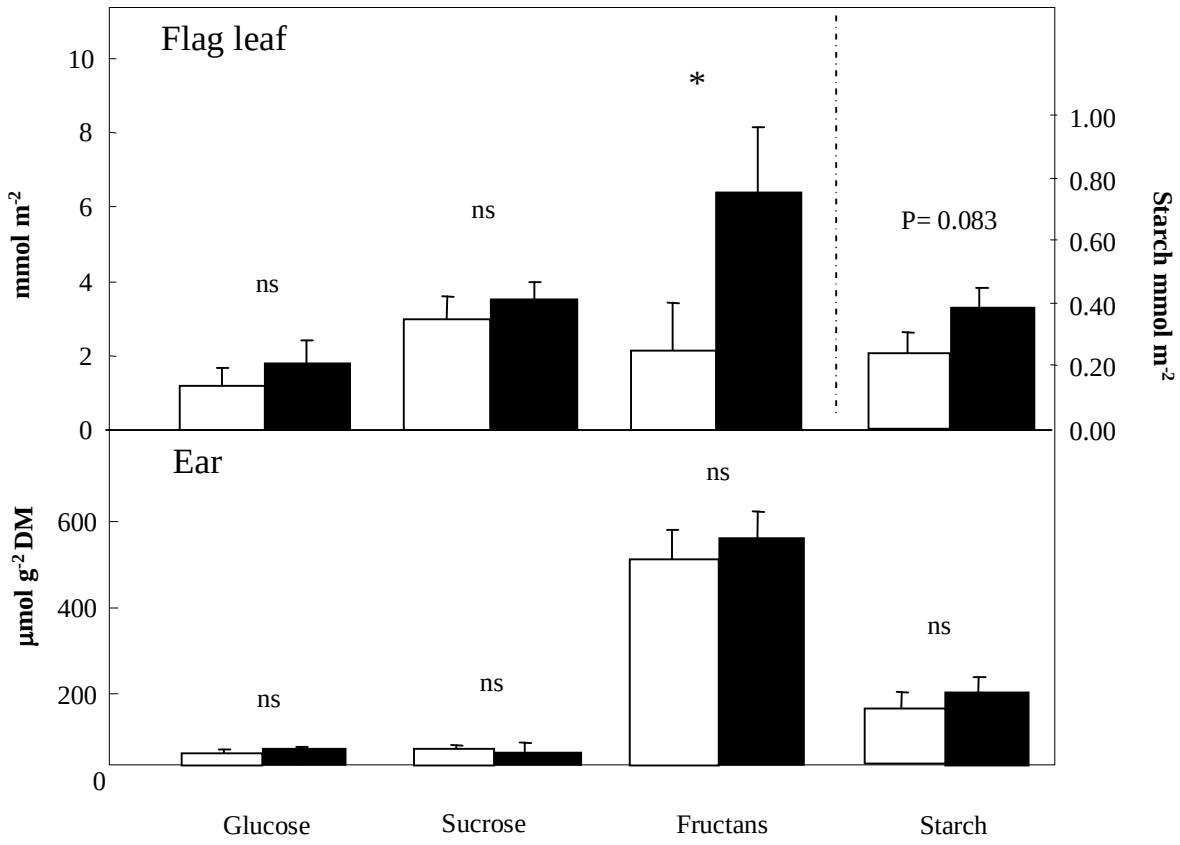
Flag leaf
Ear
mmol m-2
µmol g-2 DM
Starch mmol m-2
10
8
6
4
2
0
600
400
200
0
1.00
0.80
0.60
0.40
0.20
0.00
ns
ns
*
P= 0.083
ns
ns
ns
ns
Glucose
Sucrose
Fructans
Starch

Figure 2

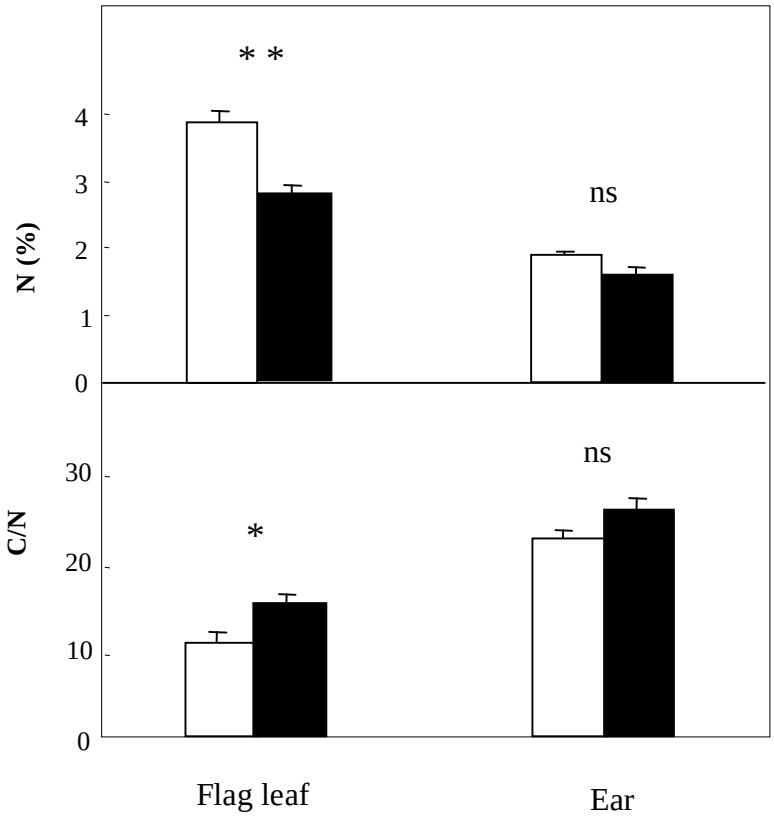

Figure 3

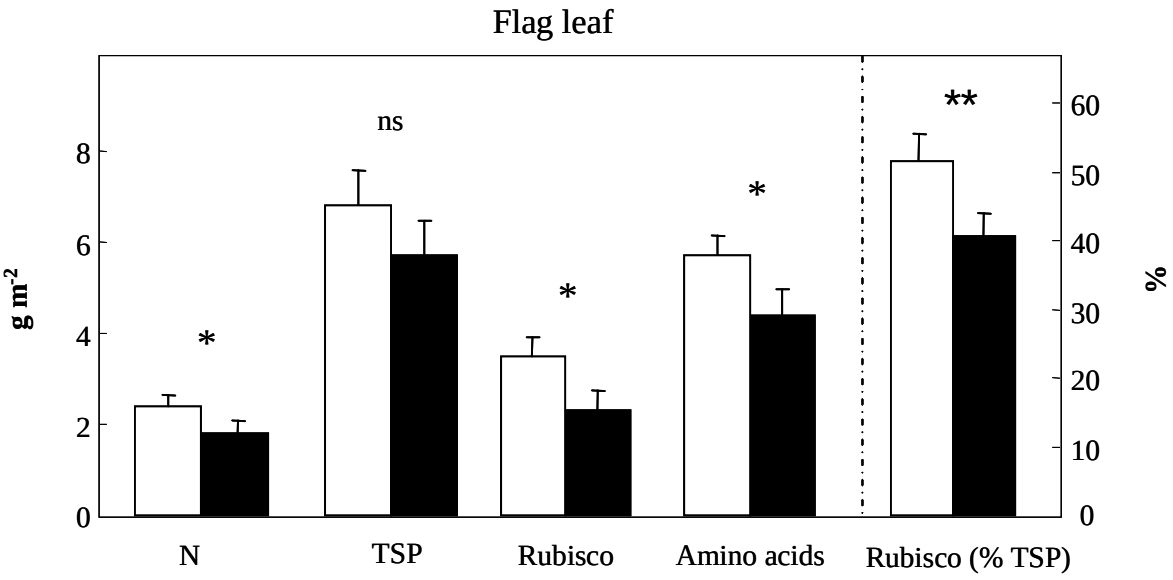
Flag leaf
g m-2
%
0
2
4
6
8
0
10
20
30
40
50
60
*
ns
*
*
**
N
TSP
Rubisco
Amino acids
Rubisco (% TSP)

Figure 4

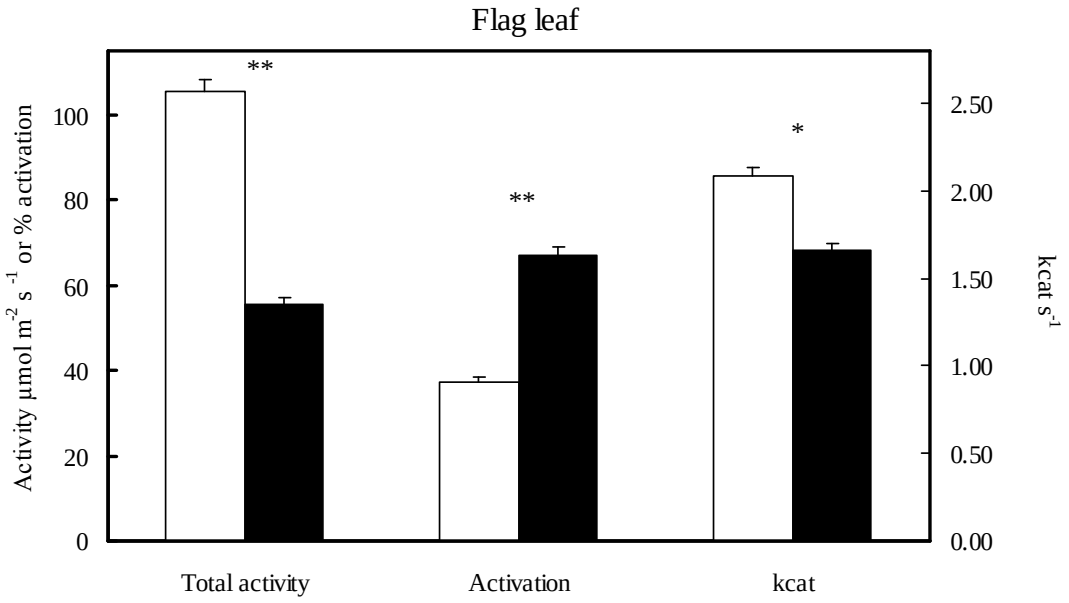
Flag leaf
Activity µmol m-2 s-1 or % activation
kcat s-1
0
20
40
60
80
100
0.00
0.50
1.00
1.50
2.00
2.50
**
**
*
Total activity
Activation
kcat

Figure 5

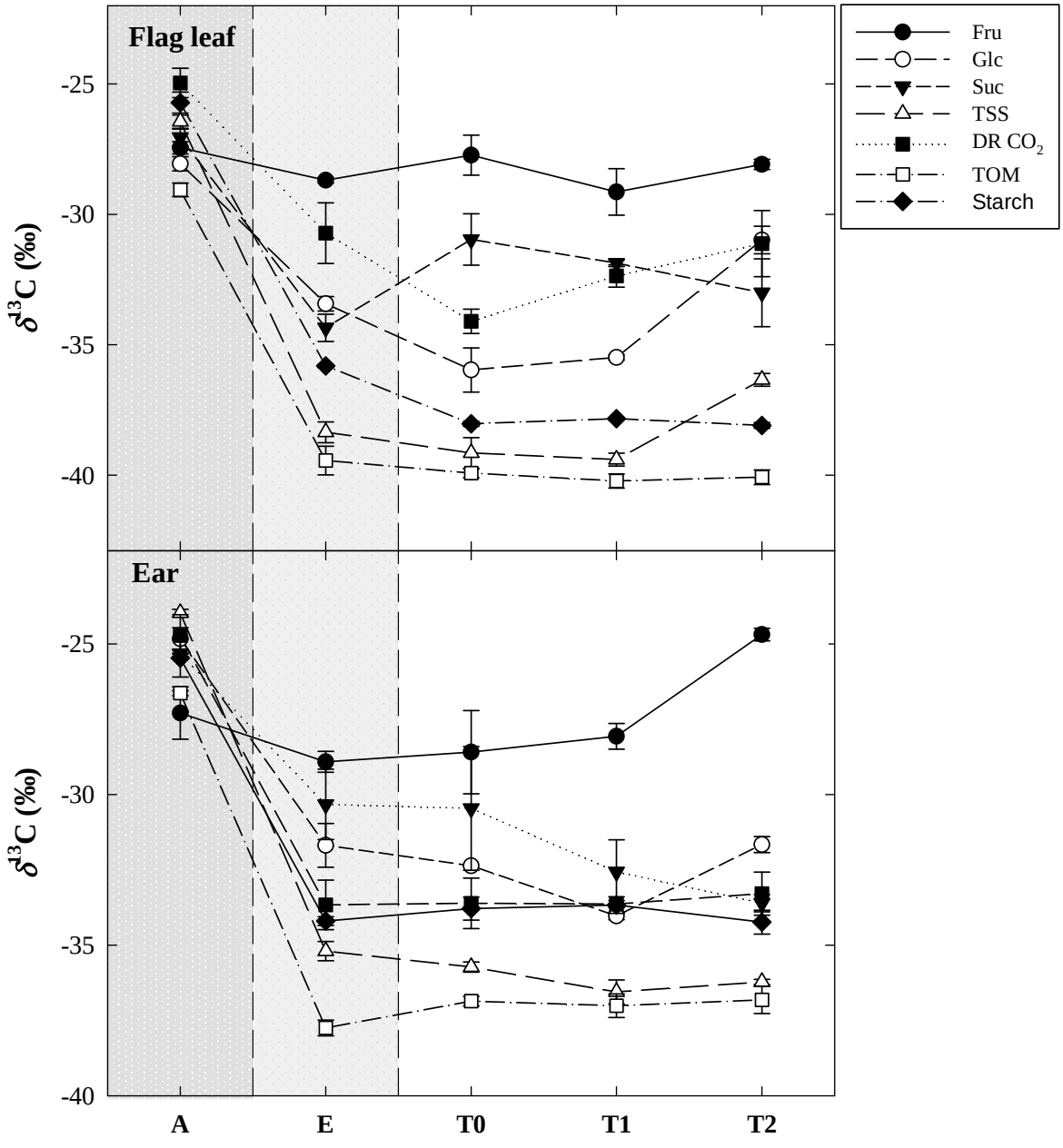
Flag leaf
Ear
Fru
Glc
Suc
TSS
DR CO2
TOM
Starch
δ13C (‰)
-25
-30
-35
-40
A
E
T0
T1
T2

Figure 6

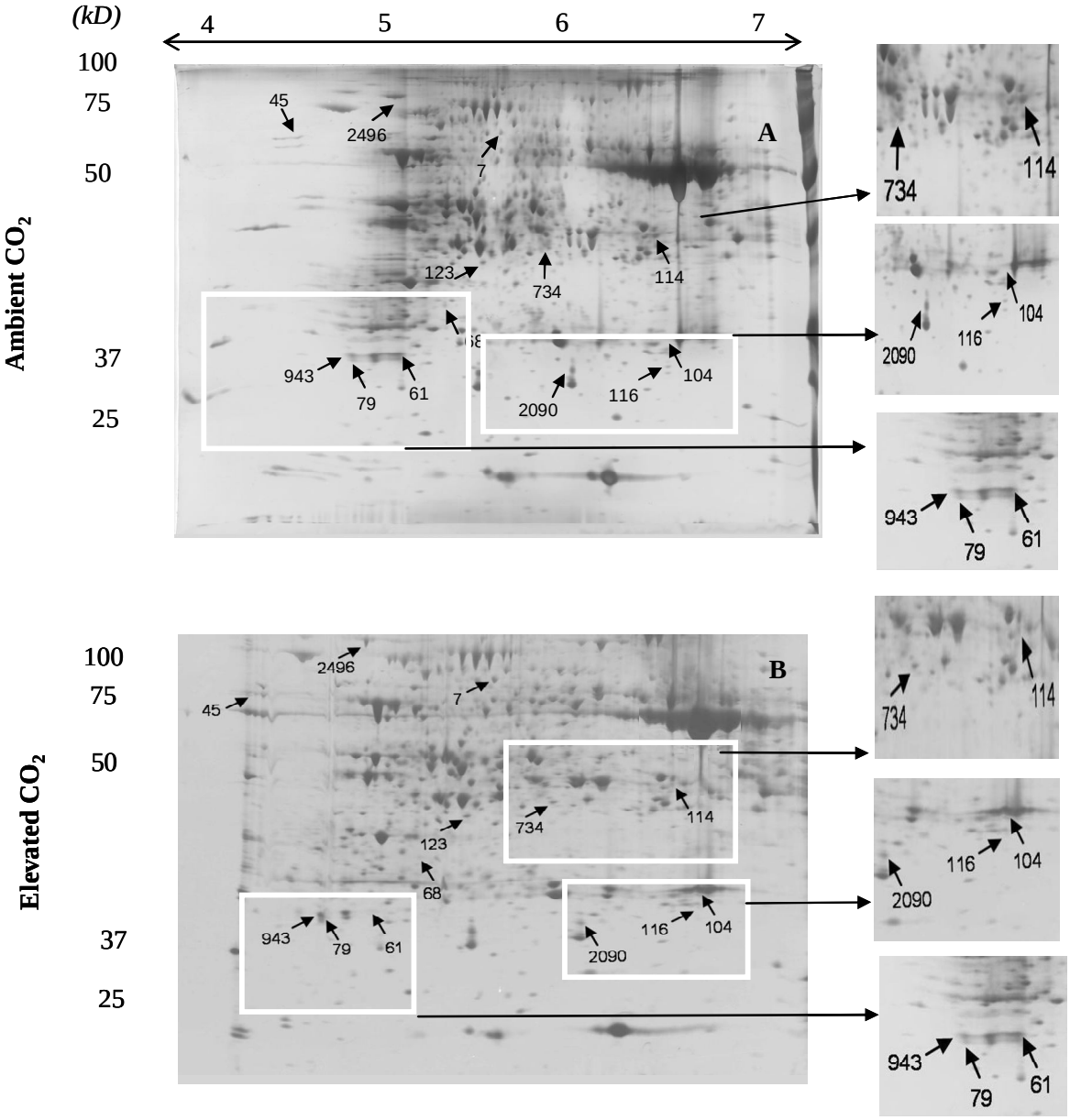
(kD)
4
5
6
7
100
75
50
37
25
Ambient CO_2
45
2496
7
A
123
734
114
943
79
61
2090
116
104
Elevated CO_2
B
68

Table 1

Effect of [CO_2] during growth on wheat total, flag leaf, ear, and ear DM/total DM, together with photosynthesis, stomatal conductance (gs) and intercellular CO_2 (Ci) determined at 370 (A_{370}, gs_{370} and Ci_{370} respectively) and 700 (A_{700}, gs_{700} and Ci_{700} respectively) μmol mol^{-1} [CO_2] 14 days after anthesis. Each value represents the mean ± SE (n= 6). The different letters indicate significant differences (P<0.05) among treatments and genotypes as determined by ANOVA test.

Parameters	**Ambient CO_2**				**Elevated CO_2**			
				Plant growth data				
Total DM (g m^{-2})	2287.1	±	510.4	a	1871.2	±	171.9	a
Flag leaf DM (g m^{-2})	92.3	±	15.3	a	73.3	±	152	a
Ear DM (g m^{-2})	662.0	±	240.0	a	426.7	±	46.9	a (F=0.093)
Ear DM/Total DM	0.29	±	0.09	a	0.23	±	0.01	a
				Gas exchange data				
A_{370} (μmol m^{-2} s^{-1})	14.59	±	5.5	a	3.77	±	0.61	b
A_{700} (μmol m^{-2} s^{-1})	33.7	±	6.0	a	21.6	±	4.4	b
gs_{370} (mmol m^{-2} s^{-1})	146.9	±	62.3	a	51.8	±	4.73	b
gs_{700} (mmol m^{-2} s^{-1})	184.3	±	46.4	a	124.0	±	35.7	b
Ci_{370} (mol mol^{-1})	153.6	±	12.7	b	277.0	±	9.90	a
Ci_{700} (mol mol^{-1})	324.5		17.6	a	345.9		78.7	a

Table 2. Annotation of elevated CO_2 **up-regulated** spots identified in silver stained two-dimensional electrophoresis gels of leaves collected 14 days after anthesis. A total of 125 µg of total proteins was loaded on an 18-cm gel strip forming an immobilized linear pH gradient from 4 to 7. Second dimension electrophoresis (SDS1258 PAGE) was carried out on 12 % polyacrylamide (w/v) gels (20 × 20 cm) (for details see ‘‘Material and Methods’’).

Spot no.	Spot % volume variations	pI/Mr	PM	SC (%)	Score ($p < 0.05$ corresponding to score > 51)	Protein name / Organism /NCBI accession no.
01. Metabolism						
104	198.03	6.25/32.01	7	28	249	Chloroplastic carbonic anhydrase gi|729003
02. Energy						
7	627.13	5.51/62.91	2	11	55	Phosphoglycerate mutase / gi|32400802
07. Transporters						
45	314.21	4.05/54.82	3	6	98	ATP synthase β subunit / gi|3850920
11. Disease/defence						
116	164.06	6.48/24.09	1	6	53	Manganese superoxide dismutase / gi|1621627
12. Unclear classification						
105	188.61	8.67/81.43	2	3	53	Putative blue light receptor / gi|20797092
123	139.12	5.35/42.85	3	3	54	SNF2 superfamily protein / gi|159466410
13. Unclassified						
79	244.27	4.42/23.86	2	2	63	Predicted protein / gi|226460198
943	195.90	4.43/24.77	4	18	122	Hypothetical protein / gi|1076722

Table 3. Annotation of elevated CO_2 **down-regulated** spots identified in silver stained two-dimensional electrophoresis gels of leaves collected 14 days after anthesis. A total of 125 µg of total proteins was loaded on an 18-cm gel strip forming an immobilized linear pH gradient from 4 to 7. Second dimension electrophores is (SDS1258 PAGE) was carried out on 12 % polyacrylamide (w/v) gels (20 × 20 cm) (for details see ‘‘Material and Methods’’).

Spot no.	Spot % volume variations	pI/Mr	PM	SC (%)	Score ($p < 0.05$ corresponding to score > 51)	Protein name / Organism /NCBI accession no.
02. Energy						
114	60.59	6.21/48.39	2	8	112	Ribulose-bisphosphate carboxylase activase / gi|100614
2090	79.12	5.81/23.97	2	5	65	Adenosine diphosphate glucose pyrophosphatase / gi|13160411
11. Disease/defence						
2496	87.75	4.91/85.64	2	3	81	Cytosolic heat shock protein 90 / gi|32765549
13. Unclassified						
61	34.66	4.95/24.65	2	9	92	Hypothetical protein / gi|1076722
68	37.85	5.20/38.94	1	91	66	Unknown protein 18 / gi|205830697
734	28.14	5.64/44.58	2	10	103	Hypothetical protein / gi|125602085